Nanoscale Advances

ROYAL SOCIETY OF CHEMISTRY

PAPER

View Article Online
View Journal | View Issue

Cite this: *Nanoscale Adv.*, 2025, **7**, 2518

Genomic nano-biosensor for rapid detection of the carbapenem-resistant gene *bla*$_{NDM-1}$ in carbapenemase-producing bacteria

Regina Kemunto Mayaka [abc] and Evangelyn C. Alocilja *[ab]

Antimicrobial resistance (AMR) has become one of the major public health concerns causing serious obstacles to the successful prevention and treatment of infectious diseases. To curb the spread of AMR, well-equipped laboratories for the early detection of disease-causing pathogens and resistant genes are crucial, something that remains unmet in developing countries due to resource constraints and inadequate infrastructure. This paper presents an affordable and simple nanoparticle-based biosensor for rapidly detecting the *bla*$_{NDM-1}$ gene in carbapenemase-producing (CP) bacteria. The biosensor employs thiol–ligand surface functionalized gold nanoparticles (GNPs) conjugated with an oligonucleotide probe specific for detecting the *bla*$_{NDM-1}$ gene. The biosensor was evaluated using DNA extracted from CP bacteria having the target *bla*$_{NDM-1}$ gene, two non-NDM-1 CP bacteria, and five susceptible bacterial strains. Tuning of the localized surface plasmon resonance (LSPR) of the GNPs was achieved by reducing the surrounding pH of the GNPs, hence inducing aggregation. With the binding of GNPs–probe–target DNA, the stability of GNPs was enhanced, as confirmed by the retention of the red colour when an optimized amount of 0.1 M HCl was added to induce aggregation. The absence of target DNA was indicated by the aggregation of GNPs after the addition of acid, which resulted in a colour change from red to blue/purple and a shift in the LSPR band to a longer wavelength, averaging 620 nm. The biosensor visual detection results were quantified with absorbance spectra measurements and the results were achieved within 30 minutes. The biosensor successfully detected the target DNA from *bla*$_{NDM-1}$ positive bacteria and distinguished the non-targets. The analytical sensitivity achieved was 2.5 ng μL^{-1} which corresponds to approximately 10^3 colony-forming units per milliliter. These findings were confirmed through PCR amplification. This nano-biosensor offers an inexpensive, simple, rapid, and sensitive method for detecting the *bla*$_{NDM-1}$ gene in carbapenemase producers, and is readily implementable in resource-limited settings.

Received 24th September 2024
Accepted 21st February 2025

DOI: 10.1039/d4na00798k

rsc.li/nanoscale-advances

1 Background

Early detection of pathogenic bacteria and their resistance genes is a crucial factor in healthcare and overall public health. Antimicrobial resistance (AMR) is one of the most worrying public health concerns challenging the world today.[1] Indiscriminate use of antibiotics in medical care, agriculture, and veterinary care has resulted in selection pressure favouring the survival and spread of such resistant microorganisms, leading to prolonged hospital stays, high morbidity, and mortality.[2,3] An estimated 700 000 people lose their lives to AMR infections annually and this number is projected to reach 10 million by 2050, according to the US Centers for Disease Control and Prevention (CDC).[4] However, despite the advent of effective antibiotic therapy, bacteria continue to mutate to evade the treatment programs in question, giving rise to a global threat.[5,6]

Carbapenems play a significant role in the antibiotic landscape, as they offer the broadest spectrum of activity and highest potency among β-lactam antibiotics. They are the most widely used drugs to treat bacterial infections due to their safety and efficacy.[7,8] However, the expression of β-lactamase genes is one of the mechanisms by which pathogens become antibiotic resistant. These pathogens produce carbapenemase-type β-lactamase enzymes, which neutralize the lethal action of the antibiotics; thus, they have been identified as critical priority pathogens by the World Health Organization (WHO).[9,10] They include a serine-β-lactamase type *Klebsiella pneumoniae* carbapenemase (KPC) and metalloid-β-lactamase types, such as Imipenemase (IMP), Verona integrin encoded metalloid β-lactamase (VIM), and New Delhi metallo-lactamase (NDM) carbapenemases.[8] The New Delhi metallo-lactamase (NDM) was first identified in 2009 in *Klebsiella pneumoniae* and *Escherichia coli* isolated from a patient in Sweden who had previously been hospitalized in New Delhi, India.[11,12] To date, there are twenty-

[a]*Department of Biosystems and Agricultural Engineering, Michigan State University, East Lansing, MI 48824, USA. E-mail: alocilja@msu.edu*

[b]*Global Alliance for Rapid Diagnostics, Michigan State University, East Lansing, MI 48824, USA*

[c]*Department of Chemistry, Egerton University, Nakuru 536-20115, Kenya*

eight NDM variants classified as NDM-1 through NDM-28, with NDM-1 and NDM-5 being commonly detected in *Enterobacterales*.[13,14]

NDM-1 is the most common variant in clinical infections, and the gene that encodes β-lactamase, $bla_{\text{NDM-1}}$, has rapidly spread to different Gram-negative pathogenic species worldwide since its detection, through transfer of the $bla_{\text{NDM-1}}$ gene among mobile plasmids and clonal outbreaks.[15,16] Even though $bla_{\text{NDM-1}}$-containing bacteria display severity like other enterobacteria, they are resistant to a broad spectrum of β-lactam antibiotics, including carbapenems, penicillins, and cephalosporins.[17] A scenario that is threatening to public health is the existence of NDM-1 genes, which have been detected in the food chain [18,19] and several compartments of the environment: hospital sewage,[20] drinking tap water,[21] and municipal waste water.[22]

Effective prevention of the spread of NDM-1 producers requires a rapid screening assay that can detect the NDM-1 gene in food, water and the environment early enough.[23,24] In addition, to reduce the misuse of antibiotics, a fast, robust, and affordable antimicrobial susceptibility test (AST) is imperative, as about 50% of antibiotic treatments are initiated with wrong antibiotics and without proper pathogen detection.[25]

AST assays presently used in medical practice for carbapenemase detection include growth-based assays, which measure carbapenem resistance based on the growth of bacteria in the presence of a carbapenem antibiotic, namely the modified Hodge test and the modified carbapenem inactivation method.[26,27] Secondly, hydrolytic methods detect carbapenem degradation products, with examples including the Carba NP test and matrix-assisted laser desorption-ionization time of flight mass spectrometry (MALDI-TOF).[28,29] And thirdly, lateral flow immunoassays usually detect carbapenemase enzymes using specific antibodies.[30,31] The Carba NP test is preferred by the Clinical and Laboratory Standards Institute (CLSI) as a reliable phenotypic method for carbapenemase detection.[32] However, these phenotypic methods are time-consuming and sometimes, costly in terms of equipment and supplies.[33,34]

Genotypic AST identifies specific resistance genes or genetic mutations using molecular or genomic DNA amplification.[35] Polymerase Chain Reaction (PCR)-based methods, whole genome sequencing (WGS), loop-mediated isothermal amplification (LAMP), DNA microarray and chips, and fluorescence *in situ* hybridization (FISH) are some of the genotypic techniques for the detection of these resistant genes.[34] Real-time PCR methods capable of detecting bla_{NDM}-positive isolates directly from clinical samples have been reported.[36] The PCR method allows the exponential amplification of specific sequences of DNA and RNA. Additionally, a high specificity, fast and dependable multiplex PCR technique for the rapid screening of carbapenemase genes has been developed.[37,38]

In general, genotypic methods are recognized for being rapid, sensitive, explicit, and specific in detection of resistance genes. Nevertheless, they also have drawbacks including expensive equipment and reagents, as well as the need for skilled personnel, decreasing their clinical utility,[39–41] especially in resource constrained regions. Thus, a timely and accurate detection method for resistant genes is particularly important for the control of the spread and treatment of infections.[42] Biosensors have emerged as specific, sensitive, and cost-effective techniques for early-stage diagnosis, a fundamental aspect of health care management,[43] and they come in various forms.[44] Among them, a novel electrochemical biosensor was developed to detect the drug-resistant gene $bla_{\text{NDM-1}}$.[17] In another study, a thermometric NDM-1 biosensor enabled the detection of β-lactamases (metallo- and serine-carbapenemases) in clinical bacterial isolates with 100% accuracy.[45] Similarly, a disposable lateral flow biosensor detected *A. baumannii* strains harboring the $bla_{\text{OXA-23}}$-like gene with a specificity of 100%.[46]

The unique and highly tunable optical properties, high surface area to volume ratio and chemical stability of gold nanoparticles (GNPs) have shown enormous potential in the development of state-of-the art biosensing techniques. In addition, their ease of modification with a wide variety of thiol-terminated organic biomolecules through the formation of strong Au–S bonds and ligand exchange reactions, leads to stable colloidal suspensions in aqueous solutions.[47]

A GNP-based biosensor is based on the principle of localized surface plasmon resonance (LSPR), giving rise to a strong absorption band in the visible region. A bathochromic resonance/wavelength shift occurs due to changes in interparticle distance.[48,49] The pH change leads to modification in the dielectric properties triggering the aggregation of GNPs resulting in a shift of the LSPR band from 520 to 620 nm and a change in the colour of the colloidal solution from wine red (dispersed) to purple/blue (aggregated) due to interparticle surface plasmon coupling.[47] GNP-based optical biosensors have enormous potential to be used as point-of care devices owing to their cost-effectiveness, high sensitivity, and reliable analytical results. A plasmonic nano-biosensor able to detect CP pathogens directly from urine within 2.5 hours has been reported previously.[50] In a more recent study, a dextrin-coated GNP-based, genomic plasmonic biosensor has been developed for the detection of the KPC-producing carbapenem-resistant bacteria in 30 min.[51]

In this research paper, we describe a rapid, cost effective, simple, visual and label free GNP-based nano-biosensor for the detection of the NDM-1 gene expressed by CP bacteria. The biosensor is applicable in environmental surveillance and in clinical diagnostics.

1.1. Novelty of the research study

The nano-biosensor was designed to detect the NDM-1 resistant gene in CP bacteria. The novelty of the study lies in the use of a 50-mer oligonucleotide probe specific for detecting the NDM-1 resistant gene in CP bacteria without the need for PCR amplification. Additionally, the biosensor demonstrates the capability to monitor resistant genes in water samples.

2 Materials and methods

2.1. Materials

This study utilized eight bacterial stock cultures, including the NDM-1 resistant target strain *Escherichia coli* (BAA-2471) and non-target resistant CP strains, *Klebsiella pneumoniae* subsp.

pneumoniae (BAA-13883) and *E. coli* (BAA-2340). Additionally, two susceptible strains were procured from the American Type Culture Collection (ATCC). Three other susceptible strains were obtained as frozen cultures from the Nano-Biosensors Laboratory at Michigan State University. The DNA extraction kits were purchased from Qiagen (Germantown, MD, USA). A NanodropOne spectrophotometer from ThermoFisher Scientific (Waltham, MA, USA) was used to assess the quality and quantity of the DNA samples and measure the absorption spectra. Oligonucleotide probes were designed and ordered from Integrated DNA Technologies (IDT; Coralville, Iowa). Phosphate Buffer Saline (PBS), Nutrient Agar (NA) and Nutrient Broth (NB), Hydrochloric acid (HCl), gold(III) chloride ($HAuCl_4$), sodium carbonate (Na_2CO_3), 11-mercaptoundecanoic acid (MUDA: $HS(CH_2)_{10}CO_2H$), sodium dodecyl sulfate (SDS, $CH_3(CH_2)_{11}OSO_3Na$) and dextrin from potato starch were purchased from Sigma Aldrich (St. Louis, MO, USA).

2.2. Bacterial strains

The bacterial strains utilized in this study are detailed in Table 1.

2.3. DNA extraction

Overnight bacterial cultures from various strains were used to extract DNA with a Qiagen kit. The extracted DNA was then suspended in elution buffer (pH 8). The concentration and quality of the extracted DNA were measured using a Nanodrop spectrophotometer, with acceptable quality ratios for A260/A280 being approximately 1.8 and for A260/A230 being around 2.0. These DNA samples were then used for the biosensor assay. Additionally, overnight fresh bacterial cultures grown in nutrient broth (NB) were used to inoculate the water samples. The strains included the target NDM-1 positive *E. coli* strain and the non-target strains *E. coli* C3000 and enterotoxigenic *E. coli*, ETEC. Uncontaminated samples were used as negative controls representing the natural microflora. To artificially contaminate the water samples, 1 mL of 10^3 CFU mL^{-1} from serially diluted overnight bacterial culture was added to 25 mL of tap water samples. They were left to acclimatize for 1 h at room temperature before 225 mL of PBS was added to each sample. A volume of 100 mL was transferred into 100 mL Whirl Pak bags, followed by addition of 1 mL of MNP to the bag. They were mixed, and allowed to incubate at room temperature for 5 min. The Whirl Pak bag was then attached to a magnetic rack for another 5 min before supernatant removal. The remaining sample was resuspended in 1 mL of PBS. For each concentrated sample, 500 μL was then transferred to 4.5 mL of NB and incubated for 12 h. DNA was then extracted using a Qiagen kit and quantified using a Nanodrop spectrophotometer. DNA samples extracted from target-inoculated water, two non-target-inoculated samples, and uncontaminated water were used for biosensor tests.

2.4. Synthesis of dextrin capped GNPs and surface modification

Dextrin-capped gold nanoparticles (GNPs) were synthesized under alkaline conditions using a greener method as previously described by Anderson *et al.*[52] In brief, gold(III) chloride trihydrate was dissolved in distilled sterile water and reduced under alkaline conditions by adding sodium carbonate. Dextrin was then added, and the hot plate was heated to 150 °C. The solution temperature was maintained between 90 and 95 °C for 30–60 minutes under continuous stirring until it turned wine red. The absorption maximum at approximately 520 nm (wine red colour) of the synthesized GNPs was then confirmed using a Nanodrop UV-vis spectrophotometer. The GNPs were then surface functionalized with 25 μM 11-mercaptoundecanoic acid (MUDA) and suspended in 0.1 M borate buffer. For biosensor applications, MUDA functionalization allows for amine–thiol ligand interaction, and the oligo probe then hybridizes with the target DNA, to form a stable GNP–probe–DNA complex. The ready-to-use surface-modified GNPs were stored at 4 °C until further use.

2.5. Probe design

An NDM-1-specific oligonucleotide probe with a single-stranded complementary sequence was designed to target the NDM-1 gene in carbapenemase-producing (CP) bacteria. The probe was designed using the bla_{NDM-1} gene sequence of carbapenem-resistant *E. coli* (ATCC BAA-2471), utilizing the design tools from the National Center for Biotechnology Information (NCBI) and the Basic Local Alignment Search Tool (BLAST). The *E*-values were then checked to ensure no cross-reactivity with non-target sequences and confirm that the oligonucleotide gene sequence was specific to the NDM-1 gene. The single-stranded 50-mer aminated oligonucleotide probe, specific to the genomic DNA of the NDM-1 gene, was employed for this study: 5′-CAACA-CAGCCTGACTTTCGCCGCCAATGGCTGGGTCGAACCAG-CAACCGC-3′. The probe was aminated at the 5′ end. A C6 hexyl linker was used to attach the amine group to the probe,

Table 1 Bacterial strains and description

Strain name	Description	Category
Escherichia coli BAA-2471	NDM-1 producing resistant strain	Resistant
Klebsiella pneumoniae subsp. *pneumoniae* (BAA-13883)	KPC-producing resistant strain	Resistant
Escherichia coli (BAA-2340)	KPC-producing resistant strain	Resistant
Escherichia coli C-3000 (BAA-15597)	Susceptible strain	Susceptible
Enterotoxigenic *Escherichia coli* (BAA-35401)	Susceptible strain	Susceptible
Vibrio cholerae (BAA-2163)	Susceptible strain	Susceptible
Salmonella enterica serotype *Typhimurium*	Susceptible strain	Susceptible
Salmonella enterica serovar *Enteritidis*	Susceptible strain	Susceptible

Table 2 Bacterial strains examined for the specificity test

Positive target	Negative non-target (non-NDM-1) KPC-producing bacteria	Negative non-target susceptible bacteria
E. coli (BAA-2471)	*K. pneumoniae* (BAA-13883) *E. coli* (BAA-2340)	*E. coli* C3000 *E. coli* ETEC *Salmonella* (2) *V. cholerae*

providing flexibility and preventing steric hindrance during hybridization. This 50-mer probe was chosen to balance specificity and sensitivity. Preliminary studies in our lab demonstrated that shorter probes, while offering higher sensitivity, suffered from lower specificity. Conversely, longer probes exhibited greater specificity but at the expense of sensitivity. Thus, a 50-mer length was selected to optimize both aspects. Additionally, the probe was meticulously designed to avoid cross-reactivity with non-target sequences, ensuring accurate and reliable detection of the NDM-1 gene. The PCR primer sequence used for validation of results was F-5′ GGTTTGGCGATCTGGTTTTC and R-5′ CGGAATGGCTCATCACGATC using the protocol adapted from a previous study.[53] The amplified DNA from different samples was analysed on a 2% agarose gel in Tris Acetate EDTA (TAE) buffer at an applied voltage of 120 V for 1 h.

2.6. Biosensor design and optimization

The biosensor design was adapted from an earlier study by Dester *et al.*[54] First, the DNA from the bacterial inoculum was extracted using a commercial kit. For each repeated biosensor trial, 5 μL of 25 μM DNA probe, 5 μL of GNPs, and 10 μL of DNA sample were mixed in a single tube. The tubes were then placed in a thermocycler (acting as a heating block) to allow for DNA denaturation at 95 °C for 5 min, probe annealing at 55 °C for 10 min, and then cooling for 5 min at 25 °C. Upon hybridization, an optimized amount of 0.1 M HCl was used to aggregate the GNPs after a specified optimized response time. In the presence of the target DNA, the red colour of the GNP–probe–DNA complex was maintained while in its absence, the GNPs aggregated, turning blue/purple. The colour change of GNPs was observed visually, and by measuring their light absorption using a spectrophotometer in a wavelength range of 400 nm to 800 nm. The observed visual results were quantified using the absorbance ratio at 520 nm and 620 nm.

2.7. Analytical sensitivity test

The biosensor sensitivity was evaluated at different DNA concentrations ranging from 20 to 1.25 ng μL^{-1} to determine the minimum detectable DNA concentration. For each test, both the target and non-target DNA samples were serially diluted to the desired concentration. And then, a series of nine trials using the target NDM-1 positive was compared with a susceptible non-target sample (*E. coli* C-3000). The observed colour changes and absorption measurements were used to verify the difference in GNP aggregations between the two samples. The $A_{520/620}$ values were statistically analysed at a 95% confidence interval. The sensitivity of the biosensor was determined by the lowest DNA concentration it could detect.

2.8. The specificity tests

The biosensor was validated by evaluating DNA samples of seven non-target bacterial strains, including 5 susceptible and 2 resistant KPC-producing strains. A DNA concentration of 20 ng μL^{-1} was used for all the DNA samples for each set of nine trials. Each specificity trial included a negative control (DNA-free), targets (NDM-1 positive), and non-target (NDM-1 negative) samples. Their absorbance spectral measurements and images were collected during the experiment. The differences in $A_{520/620}$ values between target and non-target samples were analysed at a 95% confidence interval. Table 2 presents a list of the strains of bacteria used for specificity tests.

2.9. Statistical analysis

Statistical analysis was conducted at a 95% confidence interval level ($\alpha = 0.05$) and the absorbance ratio at 520 nm to 620 nm corresponding to the peak absorbance of the target and non-target DNA samples was compared. All the experiments in this study were performed in 9 trials and results were reported as averages and standard deviations. Differences in group means for specificity and sensitivity were analysed by using the One-way Analysis of Variance (ANOVA) and Tukey's HSD (Honestly significant difference) test.

3 Results and discussion

3.1. The working principle of the NDM-1 nano-biosensor

The biosensor concept in this study relies on the shift in Localized Surface Plasmon Resonance (LSPR) of gold nanoparticles (GNPs), causing their aggregation and resulting in a visual colour change. This phenomenon was confirmed through spectrophotometric measurements. GNP aggregation is a consequence of uneven distribution of electrostatic repulsion, leading to a shift in their absorption maxima due to the distance-dependent nature of the LSPR. The biosensor employed alkaline-synthesized dextrin capped and 11-mercaptoundecanoic acid surface functionalized GNPs, which have an absorption peak at around 520 nm as displayed in Fig. 1a and b. The particle size ranged from 20–30 nm, as previously determined using transmission electron microscopy (TEM). Furthermore, the hybridized GNP–probe–DNA sample complex

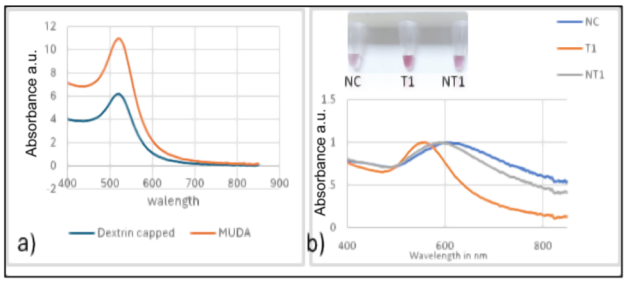

Fig. 1 (a) Absorbance spectra for dextrin coated and MUDA surface functionalized GNPs. (b) Normalized absorbance spectra for the NDM-1 biosensor at 20 ng μL^{-1}: the inset shows a visual image NC (nuclease free water), T1-target *E. coli* and NT1 non-target *E. coli* C3000.

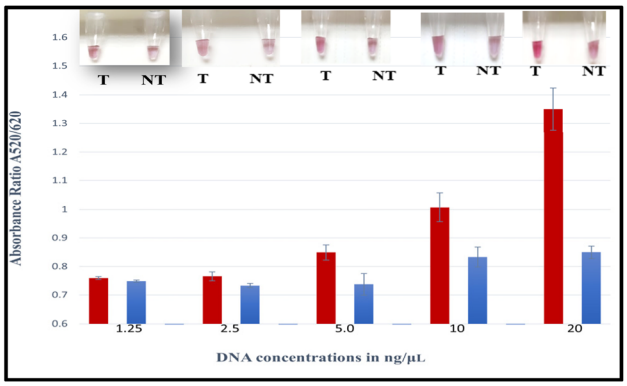

Fig. 2 Analytical sensitivity assessment: $A_{520/620}$ absorbance ratios for target *E. coli* 2471 (red bars-T) and non-target *E. coli* C3000 (blue bars-NT) at 1.25–20 ng μL^{-1}, with each concentration tested in 9 trials. The inset shows the visual results.

showed no shift in the absorbance maxima for the gold nanoparticles, indicating that the GNPs remained stable after undergoing the hybridization process in the thermocycler.[55,58] This stability suggests that the biological probe molecule retains its biorecognition properties.

3.2. Biosensor optimization

The biosensor operates on the principle of a LSPR absorption peak shift, which occurs due to the aggregation of gold nanoparticles (GNPs). This aggregation is visually indicated by a colour change from red to blue or violet. This was quantified spectrophotometrically on a Nanodrop spectrophotometer. In this study, we utilized the GNPs' absorption peak at around 520 nm and observed a shift in the peak maximum to approximately 620 nm. The optimization parameters involved the amount of HCl added and the time between HCl addition and visual response measurement, which were then quantified by spectroscopic measurements. The optimized parameters resulted in the optimal and most consistent bathochromic peak shift difference between target and non-target analytes along with a clearly visible red target sample when compared to the purple/blue non-target and control. The optimization procedure determined that 7 µL of 0.1 M HCl and a 10 min response time were optimal. As previously reported,[51,54,55] the biosensor assay, from sample preparation to colour change assessment, could be completed in approximately 30 min.

3.3. Analytical sensitivity of the nano-biosensor

The lowest DNA concentration detected by the biosensor was evaluated using target DNA (resistant *E. coli*) and the non-target DNA (susceptible *E. coli* C3000). The DNA samples for both the target and non-target were diluted by a factor of two, ranging from 20 to 1.25 ng μL^{-1}.

The colour of the target and non-target DNA samples at similar concentrations was visually assessed and compared with absorbance spectral measurements.

Fig. 1b depicts the absorbance spectra of the biosensor at 20 ng μL^{-1} with an inset image showing the colour differences for the negative control NC (water free of DNA), the target T and the non-target NT (*E. coli*). For the nine trials, there was an average clear shift of ≈100 nm to a longer wavelength for the negative control NC and the non-target. The target exhibited a minimal shift, thereby retaining the red colour as observed visually in the inset photo and evidenced by a narrower band in the absorbance spectrum Fig. 1b.

The absorbance measurements for each comparable concentration were quantified and compared with the colour change. The absorbance ratio $A_{520/620}$ of GNP–probe–DNA complex aggregation was also used to show the differences between the target and non-targets. The tube images together with the absorbance ratios ($A_{520/620}$) of the target and non-targets are displayed in Fig. 2.

High absorbance ratios were realized for target samples for each sample concentration assessed, indicating minimum aggregation. Samples that exhibited lower absorbance ratios were non-targets. The mean differences of $A_{520/620}$ for the target and non-target DNA samples were also plotted as a function of the different DNA concentrations as demonstrated in Fig. 3. It was observed that at a concentration of 20 ng μL^{-1}, the difference in the absorbance ratio between the target and non-target samples was the highest, followed by concentrations of 10, 5 and 2.5 ng μL^{-1}, respectively.

The statistical mean differences between target and non-target samples for each concentration were evaluated using ANOVA followed by Tukey's test at a 95% confidence level. The differences between the target and non-target samples at 20, 10,

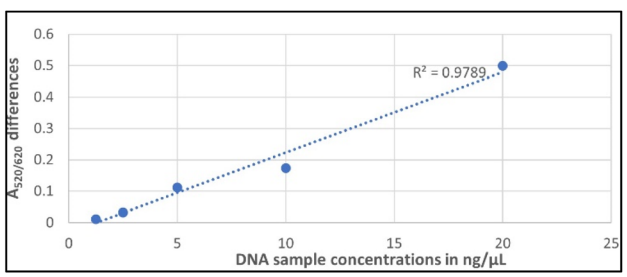

Fig. 3 A linear graph showing the linearity of $A_{520/620}$ differences between the target and non-target samples against concentration (ng μL^{-1}).

5, and 2.5 ng μL^{-1} were found to be significantly different ($\rho < 0.05$) at a 95% confidence interval. The observed $A_{520/620}$ difference at 2.5 ng μL^{-1} was minimal, however, there was a significant difference between the target and non-target sample ($\rho < 0.05$). Whereas at 1.25 ng μL^{-1} there was no significant difference ($\rho > 0.05$), nor a clear visual colour distinction between the target and non-target sample as shown in Fig. 2. The analytical sensitivity for the biosensor was therefore identified as 2.5 ng μL^{-1} corresponding to $\sim 10^3$ CFU mL^{-1}, substantiating recent findings for a nanoparticle-based plasmonic biosensor for detecting the *Klebsiella pneumoniae* (bla_{KPC}) gene in CP strains.[51] Other colorimetric assays reported lower sensitivities. For instance, a genomic biosensor for detecting *E. coli* C3000 had a detection limit of 10 ng μL^{-1}.[55] Likewise, a colorimetric biosensor using an SEB-binding aptamer (SEB2) and unmodified GNPs for the detection of *Staphylococcal enterotoxin* B (SEB) had a sensitivity of 50 ng μL^{-1} for visual detection.[56] Other assays from the literature include an LSPR-based label free aptasensor designed to detect whole-cell multidrug resistant *Pseudomonas aeruginosa* strain PAO1 that was found to have a limit of detection of 10 CFU mL^{-1} with ~3 h detection time.[57] An earlier study of a plasmonic nano sensor for a bedside detection of CP producing pathogens demonstrated higher detection limits of $>10^5$ CFU mL^{-1}.[50]

3.4. Specificity of the nano-biosensor

Seven non-target bacterial strains, including two CP producing bacteria, were evaluated for specificity studies for the bla_{NDM-1} resistant gene. The results were validated for the presence or absence of the bla_{NDM-1} gene by PCR amplification as shown in Fig. 4 and 5 below. Fig. 4a and b show the biosensor, successfully distinguishing all the susceptible strains as negative non-targets (NT1-NT5). Nuclease-free water was used as a negative control (NC). The colour change for the non-targets was visually differentiated as shown in the inset image of Fig. 4a. The mean absorbance ratios $A_{520/620}$ for the target (red bars) and the non-target samples (blue bars) at 20 ng μL^{-1} were significantly different ($\rho < 0.05$) at a 95% confidence interval. The absorbance

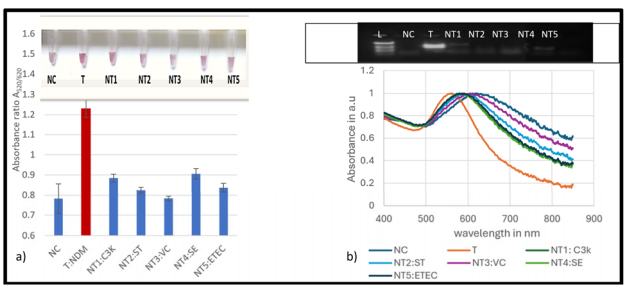

Fig. 4 Specificity results from nine trials at 20 ng μL^{-1} for the nano-biosensor using the bla_{NDM-1} probe for tested non-target susceptible strains: (a) mean absorbance ratios $A_{520/620}$ of the negative control NC, target (T) *E. coli*-BAA 2471 and non-targets (NT1; *E. coli* C3000, NT2; *S. typhimurium*, NT3; *Vibrio cholerae*, NT4; *S. enteritidis*, NT5; *Enterotoxigenic E. coli*); inset: visual detection. (b) Normalized absorbance spectra and inset: PCR amplification results of the strains along with the 1000 bp ladder.

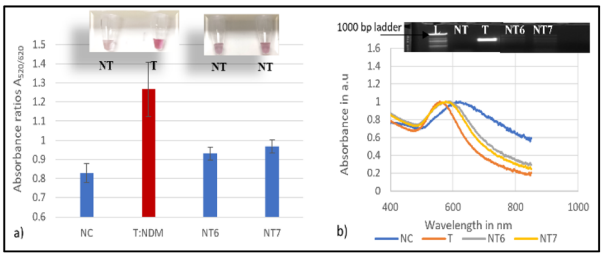

Fig. 5 Specificity results for the nano-biosensor using the bla_{NDM-1} probe. (a) Mean absorbance ratio $A_{520/620}$ of the negative control NC, target (T) and non-targets NT6 (KPC) and NT7 (KPC); the inset shows the visual images. (b) Absorbance spectra of the same strains with the inset showing the PCR amplification results along the 1000 ladder.

readings from the spectrum for the same tested strains confirmed the shift in the plasmon resonance peak on average to around 620 nm for the non-targets as observed in Fig. 4b. The validated results for the presence or absence of the bla_{NDM-1} gene by PCR amplification are shown in the inset photo of Fig. 4b. The amplification confirmed the presence of the *E. coli* BAA 2471 target DNA band, and no bands were observed for the non-targets.

Fig. 5 shows the evaluation of two non-target bacterial strains of KPC producing *K. pneumoniae* (BAA-13883 NT6) and *E. coli* (BAA-2340 NT7) using the biosensor. The visual detection results in Fig. 5a show that the biosensor positively detected the target NDM-1 and differentiated it from the non NDM-1 CP producers NT6 and NT7. The mean absorbance ratios $A_{520/620}$ for the target DNA samples and the negative control and the non-target samples (blue bars) at 20 ng μL^{-1} were significantly different ($\rho < 0.05$). This was confirmed by the absorbance peaks in Fig. 5b. The non-target and negative control samples showed broader peaks.

In summary, the designed genomic nano-biosensor assay was specific and successfully detected the NDM-1 gene target sample and distinguished the non-targets within a turnaround time of 30 min. The biosensor accurately detected the target NDM-1 CP producer and discriminated against all seven non-targets. The absorbance ratios for the target sample were in the range of 1.12–1.6, indicating that the peak shift was smaller with minimum aggregation, hence positive detection, and 0.80–0.99 for the non-targets implying a larger shift and aggregation and therefore successful differentiation. Statistical analysis using ANOVA followed by Tukey's method ($p < 0.05$) confirmed significant differences in the absorbance ratios $A_{520/620}$ between the target and all not-target samples as well as the negative control. The biosensor results were consistent with the PCR amplification results as shown in the inset of Fig. 5b.

3.5. Detection of the target bla_{NDM-1} gene from inoculated water samples using the nano-biosensor

To establish proof of concept for this biosensor's applicability in water, magnetic extraction of bacterial cells from artificially contaminated water with target *E. coli* (BAA 2471) and the non-targets *E. coli* C3000 and ETEC was conducted. The glycan

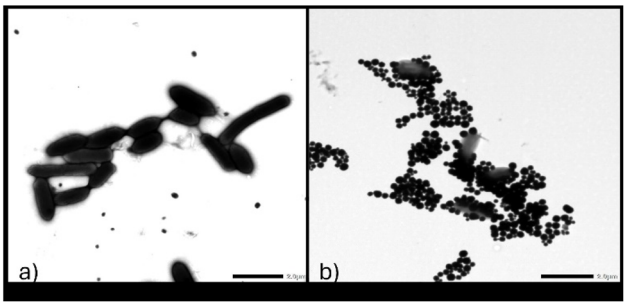

Fig. 6 TEM images of the E. *coli* BAA-2471 NDM-1 producer (a) without MNPs and (b) with MNPs.

coated magnetic nanoparticle (gMNP) enrichment step enabled the capture and concentration of the bacteria from larger volumes to smaller volumes. Successful binding between gMNPs and *E. coli* (BAA 2471) in PBS was confirmed through images from Transmission Electron Microscopy (TEM). Fig. 6 displays the TEM images of *E. coli* BAA-2471 NDM-1 producer without MNPs (Fig. 6a) and the binding of the magnetic nanoparticles with the *E. coli* resistant bacteria, thus illustrating the capture process in Fig. 6b.

The capture and concentration were followed by growth in NA and extraction of DNA from the inoculated samples. A control (NF) with no inoculation was also used to represent the natural microflora. The developed nano-biosensor assay was used to assess the DNA of the samples from water for the $bla_{\text{NDM-1}}$ resistant gene. The results of the mean absorbance ratio $A_{520/620}$ for the target and the non-targets were found to be significantly different at a 95% confidence interval as shown in Fig. 7a. These differences were validated using the absorbance readings which showed a shift in a plasmon resonance peak on average to around 620 nm for the non-targets, as shown in Fig. 7b.

However, the non-target NT5 showed a weakly correlated colour change as seen in the inset image of Fig. 7a. Nevertheless there was a significant difference in the absorbance ratio $A_{520/620}$ which was validated by PCR amplification, as shown in Fig. 7b. The biosensor can be extended to monitor food products for the presence of NDM-1, ensuring that contaminated supplies are identified and removed from the supply chain before reaching consumers. Early detection of NDM-1 in food products can prevent public health crises by allowing for rapid response and mitigation efforts. The assay offers an alternative assay for the detection of $bla_{\text{NDM-1}}$ in a short experimental time and with limited analytical equipment compared to other rapid methods that have proven to be costly and less portable.[58,59]

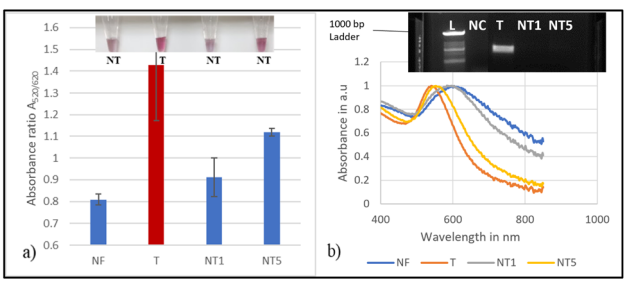

Fig. 7 (a) Mean absorbance ratios $A_{520/620}$ of the natural microflora NF, target strain (T), differentiated non-targets (NT1 *E. coli* C3000 and NT5 ETEC) from inoculated tap water and (b) absorbance spectra of same strains with the inset showing the PCR amplification results along the 1000 bp ladder.

4 Conclusions and future

A genomic-based nano-biosensor designed using GNPs stabilized by dextrin and surface functionalized with 11-mercarptoundecanoic acid notably identified the NDM-1-gene in carbapenem-resistant bacteria within 30 min. The nano-biosensor differentiated the target having the NDM-1 gene, from the non-target samples, through visual colour assessment at a low concentration of 2.5 ng μL^{-1} and a bacteria load of $\sim 10^3$ CFU mL^{-1} for the unamplified DNA samples with a turnaround time of approximately 7 h. The biosensor successfully detected the target and differentiated non-targets in water samples. For future work, this biosensor could be adapted to detect a wider range of bacterial strains in clinical, food, and environmental samples. This includes strains that carry similar resistance genes, allowing for a comprehensive assessment of its cross-reactivity profile. Moreover, integrating smartphone imaging to distinguish between aggregated and non-aggregated GNPs by identifying colour changes would eliminate the need for a spectrophotometer. This advancement would enhance the technology's applicability in low-resource settings, especially in Africa and Asia, where surveillance data are limited, and contamination of food and water is a significant concern.

Data availability

The data presented in this study are available upon request from the corresponding author.

Author contributions

Conceptualization, E. C. A. and R. K. M.; methodology, R. K. M.; validation, E. C. A, investigation, R. K. M.; formal analysis, R. K. M.; writing—original draft preparation, R. K. M.; writing—review and editing, R. K. M and E. C. A.; supervision, E. C. A.; project administration, E. C. A.; all authors have read and agreed to the published version of the manuscript.

Conflicts of interest

The authors declare no conflict of interest.

Acknowledgements

This research was supported by the Alliance for African partnership (AAP)-Michigan State University, Hatch Project 02782, and Hatch Multistate Project 04233. The authors acknowledge the Alliance for African Partnership (AAP)-Michigan State University for awarding the African Futures Program

Scholarship, and Egerton University for approving a one-year study leave. The authors express gratitude to members of the Nano-Biosensors Lab for their assistance in TEM imaging and during the initial stage of the research.

Notes and references

1 CDC, *About Antimicrobial Resistance*, 2022.
2 M. D. Barton, Antibiotic use in animal feed and its impact on human health, *Nutr. Res. Rev.*, 2000, **13**(2), 279–299, DOI: **10.1079/095442200108729106**.
3 K. L. Tang, N. P. Caffrey, D. B. Nóbrega, *et al.*, Restricting the use of antibiotics in food-producing animals and its associations with antibiotic resistance in food-producing animals and human beings: a systematic review and meta-analysis, *Lancet Planet. Health*, 2017, **1**(8), e316–e327, DOI: **10.1016/S2542-5196(17)30141-9**.
4 J. O' Neil, *Antimicrobial Resistance: Tackling a Crisis for the Health and Wealth of Nations*, 2014.
5 K. Bush and P. A. Bradford, Epidemiology of β-lactamase-producing pathogens, *Clin. Microbiol. Rev.*, 2020, **33**(2), e00047, DOI: **10.1128/cmr.00047-19**.
6 F. Perez, N. G. El Chakhtoura, K. M. Papp-Wallace, B. M. Wilson and R. A. Bonomo, Treatment options for infections caused by carbapenem-resistant Enterobacteriaceae: Can we apply "precision medicine" to antimicrobial chemotherapy?, *Expert Opin. Pharmacother.*, 2016, **17**(6), 761–781, DOI: **10.1517/14656566.2016.1145658**.
7 K. Bush and P. A. Bradford, Interplay between β-lactamases and new β-lactamase inhibitors, *Nat. Rev. Microbiol.*, 2019, **17**(5), 295–306, DOI: **10.1038/s41579-019-0159-8**.
8 K. M. Papp-Wallace, A. Endimiani, M. A. Taracila and R. A. Bonomo, Carbapenems: Past, present, and future, *Antimicrob. Agents Chemother.*, 2011, **55**(11), 4943–4960, DOI: **10.1128/AAC.00296-11**.
9 T. R. Walsh and M. A. Toleman, The new medical challenge: Why NDM-1? Why Indian?, *Expert Rev. Anti-Infect. Ther.*, 2011, **9**(2), 137–141, DOI: **10.1586/eri.10.159**.
10 M. R. Mulvey, J. M. Grant, K. Plewes, D. Roscoe and D. A. Boyd, New Delhi metallo-β-lactamase in Klebsiella pneumoniae and *Escherichia coli*, Canada, *Emerging Infect. Dis.*, 2011, **17**(1), 103–106, DOI: **10.3201/eid1701.101358**.
11 D. Yong, M. A. Toleman, C. G. Giske, *et al.*, Characterization of a new metallo-β-lactamase gene, bla NDM-1, and a novel erythromycin esterase gene carried on a unique genetic structure in Klebsiella pneumoniae sequence type 14 from India, *Antimicrob. Agents Chemother.*, 2009, **53**(12), 5046–5054, DOI: **10.1128/AAC.00774-09**.
12 K. K. Kumarasamy MPhil, P. Krishnan, M. A. Toleman, *et al.*, Emergence of a new antibiotic resistance mechanism in India, Pakistan, and the UK: a molecular, biological, and epidemiological study, *Lancet Infect. Dis.*, 2010, **10**, 597–602, DOI: **10.1016/S1473**.
13 F. Pan, Q. Xu and H. Zhang, Emergence of NDM-5 Producing Carbapenem-Resistant Klebsiella aerogenes in a Pediatric Hospital in Shanghai, China, *Front. Public Health*, 2021, **9**, 621527, DOI: **10.3389/fpubh.2021.621527**.
14 N. Farhat and A. U. Khan, Evolving trends of New Delhi Metallo-betalactamse (NDM) variants: A threat to antimicrobial resistance, *Infect., Genet. Evol.*, 2020, **86**, DOI: **10.1016/j.meegid.2020.104588**.
15 Y. M. Huang, L. L. Zhong, X. F. Zhang, *et al.*, NDM-1-producing Citrobacter freundii, *Escherichia coli*, and Acinetobacter baumannii identified from a single patient in China, *Antimicrob. Agents Chemother.*, 2015, **59**(8), 5073–5077, DOI: **10.1128/AAC.04682-14**.
16 D. van Duin and Y. Doi, The global epidemiology of carbapenemase-producing Enterobacteriaceae, *Virulence*, 2017, **8**(4), 460–469, DOI: **10.1080/21505594.2016.1222343**.
17 D. J. Diekema and M. A. Pfaller, Rapid detection of antibiotic-resistant organism carriage for infection prevention, *Clin. Infect. Dis.*, 2013, **56**(11), 1614–1620, DOI: **10.1093/cid/cit038**.
18 X. Zhu, Y. Zhang, Z. Shen, *et al.*, Characterization of NDM-1 Producing Carbapenemase in Proteus mirabilis among Broilers in China, *Microorganisms*, 2021, **9**, 2443.
19 T. H. Chaudhry, B. Aslam, M. I. Arshad, *et al.*, Emergence of bla NDM-1 Harboring Klebsiella pneumoniae ST29 and ST11 in Veterinary Settings and Waste of Pakistan, *Infect. Drug Resist.*, 2020, 3033–3043.
20 Z. Zong and X. Zhang, BlaNDM-1-carrying Acinetobacter johnsonii detected in hospital sewage, *J. Antimicrob. Chemother.*, 2013, **68**(5), 1007–1010, DOI: **10.1093/jac/dks505**.
21 K. P. Chung, S. P. Tseng, Y. T. Huang, T. H. Tsai, L. J. Teng and P. R. Hsueh, Arrival of Klebsiella pneumoniae carbapenemase (KPC)-2 in Taiwan, *J. Antimicrob. Chemother.*, 2011, **66**(5), 1182–1184, DOI: **10.1093/jac/dkr025**.
22 Y. Luo, F. Yang, J. Mathieu, D. Mao, Q. Wang and P. J. J. Alvarez, Proliferation of Multidrug-Resistant New Delhi Metallo-β-lactamase Genes in Municipal Wastewater Treatment Plants in Northern China, *Environ. Sci. Technol. Lett.*, 2013, **1**(1), 26–30, DOI: **10.1021/ez400152e**.
23 P. Nordmann, L. Poirel, A. Carrër, M. A. Toleman and T. R. Walsh, How to detect NDM-1 producers, *J. Clin. Microbiol.*, 2011, **49**(2), 718–721, DOI: **10.1128/JCM.01773-10**.
24 C. Jans, E. Sarno, L. Collineau, L. Meile, K. D. C. Stärk and R. Stephan, Consumer Exposure to Antimicrobial Resistant Bacteria From Food at Swiss Retail Level, *Front. Microbiol.*, 2018, **9**, 362, DOI: **10.3389/fmicb.2018.00362**.
25 A. Vasala, V. P. Hytönen and O. H. Laitinen, Modern Tools for Rapid Diagnostics of Antimicrobial Resistance, *Front. Cell. Infect. Microbiol.*, 2020, **10**, 308, DOI: **10.3389/fcimb.2020.00308**.
26 S. Fan, Y. Dai, L. Hou and Y. Xu, Application value of triton x-100 to modified hodge test and carbapenem inactivation method in the detection of acinetobacter baumannii carbapenemase, *Infect. Drug Resist.*, 2020, **13**, 4283–4288, DOI: **10.2147/IDR.S281049**.
27 A. Amjad, M. Ia, A. Sa, U. Farwa, N. Malik and F. Zia, Modified Hodge Test: A Simple and Effective Test for Detection of Carbapenemase Production, *Iran. J. Microbiol.*, 2011, **3**(4), 189.

28 I. Burckhardt and S. Zimmermann, Using matrix-assisted laser desorption ionization-time of flight mass spectrometry to detect carbapenem resistance within 1 to 2.5 hours, *J. Clin. Microbiol.*, 2011, **49**(9), 3321–3324, DOI: 10.1128/JCM.00287-11.

29 S. Bernabeu, L. Poirel and P. Nordmann, Spectrophotometry-based detection of carbapenemase producers among Enterobacteriaceae, *Diagn. Microbiol. Infect. Dis.*, 2012, **74**(1), 88–90, DOI: 10.1016/j.diagmicrobio.2012.05.021.

30 K. Borde, P. Swathi and D. Mathai, Lateral flow assay for the rapid detection of carbapenemases in Enterobacterales, *J. Acad. Clin. Microbiol.*, 2020, **22**(2), 85, DOI: 10.4103/jacm.jacm_31_21.

31 H. Boutal, A. Vogel, S. Bernabeu, *et al.*, A multiplex lateral flow immunoassay for the rapid identification of NDM-, KPC-, IMP- and VIM-type and OXA-48-like carbapenemase-producing Enterobacteriaceae, *J. Antimicrob. Chemother.*, 2018, **73**(4), 909–915, DOI: 10.1093/jac/dkx521.

32 P. D. Tamma and P. J. Simner, Phenotypic Detection of Carbapenemase-Producing Organisms from Clinical Isolates, *J. Clin. Microbiol.*, 2018, **56**, e01140, DOI: 10.1128/jcm.01140-18.

33 J. E. McLain, E. Cytryn, L. M. Durso and S. Young, Culture-based Methods for Detection of Antibiotic Resistance in Agroecosystems: Advantages, Challenges, and Gaps in Knowledge, *J. Environ. Qual.*, 2016, **45**(2), 432–440, DOI: 10.2134/jeq2015.06.0317.

34 Z. A. Khan, M. F. Siddiqui and S. Park, Current and emerging methods of antibiotic susceptibility testing, *Diagnostics*, 2019, **9**(2), 49, DOI: 10.3390/diagnostics9020049.

35 A. van Belkum, T. T. Bachmann, G. Lüdke, *et al.*, Developmental roadmap for antimicrobial susceptibility testing systems, *Nat. Rev. Microbiol.*, 2019, **17**(1), 51–62, DOI: 10.1038/s41579-018-0098-9.

36 T. Naas, A. Ergani, A. Carredr and P. Nordmann, Real-time PCR for detection of NDM-1 carbapenemase genes from spiked stool samples, *Antimicrob. Agents Chemother.*, 2011, **55**(9), 4038–4043, DOI: 10.1128/AAC.01734-10.

37 B. S. P. Galhano, R. G. Ferrari, P. Panzenhagen, A. C. S. de Jesus and C. A. Conte-Junior, Antimicrobial resistance gene detection methods for bacteria in animal-based foods: A brief review of highlights and advantages, *Microorganisms*, 2021, **9**(5), 923, DOI: 10.3390/microorganisms9050923.

38 A. Rohde, J. A. Hammerl, I. Boone, *et al.*, Overview of validated alternative methods for the detection of foodborne bacterial pathogens, *Trends Food Sci. Technol.*, 2017, **62**, 113–118, DOI: 10.1016/j.tifs.2017.02.006.

39 I. Gajic, J. Kabic, D. Kekic, *et al.*, Antimicrobial Susceptibility Testing: A Comprehensive Review of Currently Used Methods, *Antibiotics*, 2022, **11**(4), 427, DOI: 10.3390/antibiotics11040427.

40 J. Dietvorst, L. Vilaplana, N. Uria, M. P. Marco and X. Muñoz-Berbel, Current and near-future technologies for antibiotic susceptibility testing and resistant bacteria detection, *TrAC, Trends Anal. Chem.*, 2020, **127**, 115891, DOI: 10.1016/j.trac.2020.115891.

41 L. Dortet, L. Poirel and P. Nordmann, Worldwide dissemination of the NDM-Type carbapenemases in Gram-negative bacteria, *BioMed Res. Int.*, 2014, **1**, 249856, DOI: 10.1155/2014/249856.

42 X. Cui, H. Zhang and H. Du, Carbapenemases in Enterobacteriaceae: Detection and Antimicrobial Therapy, *Front. Microbiol.*, 2019, **10**, 1823, DOI: 10.3389/fmicb.2019.01823.

43 A. Haleem, M. Javaid, R. P. Singh, R. Suman and S. Rab, Biosensors applications in medical field: A brief review, *Sens. Int.*, 2021, **2**, 100100, DOI: 10.1016/j.sintl.2021.100100.

44 V. Singh, E. Kasana, J. Batra, H. Sable and R. Saxena, Antimicrobial Resistance: Mechanisms, Screening Techniques and Biosensors, *J. Pharm. Negat. Results*, 2022, 1724–1735, DOI: 10.47750/pnr.2022.13.s06.227.

45 Q. Meng, S. Liu, J. Meng, *et al.*, Rapid personalized AMR diagnostics using two-dimensional antibiotic resistance profiling strategy employing a thermometric NDM-1 biosensor, *Biosens. Bioelectron.*, 2021, **193**, 113526, DOI: 10.1016/j.bios.2021.113526.

46 S. Hu, L. Niu, F. Zhao, *et al.*, Identification of Acinetobacter baumannii and its carbapenem-resistant gene blaOXA-23-like by multiple cross displacement amplification combined with lateral flow biosensor, *Sci. Rep.*, 2019, **9**(1), 17888, DOI: 10.1038/s41598-019-54465-8.

47 P. Gaviña, M. Parra, S. Gil and A. M. Costero, Red or Blue? Gold Nanoparticles in Colorimetric Sensing, in *Gold nanoparticles-reaching new heights*, Intechopen, 2018.

48 P. Si, N. Razmi, O. Nur, *et al.*, Gold nanomaterials for optical biosensing and bioimaging, *Nanoscale Adv.*, 2021, **3**(10), 2679–2698.

49 C. Sönnichsen, B. M. Reinhard, J. Liphardt and A. P. Alivisatos, A molecular ruler based on plasmon coupling of single gold and silver nanoparticles, *Nat. Biotechnol.*, 2005, **23**(6), 741–745, DOI: 10.1038/nbt1100.

50 G. Santopolo, E. Rojo-Molinero, A. Clemente, M. Borges, A. Oliver and R. de la Rica, Bedside Detection of Carbapenemase-Producing Pathogens with Plasmonic Nanosensors, *Sens. Actuators, B*, 2021, **329**, 129059, DOI: 10.1016/j.snb.2020.129059.

51 O. Caliskan-Aydogan, S. A. Sharief and E. C. Alocilja, Nanoparticle-Based Plasmonic Biosensor for the Unamplified Genomic Detection of Carbapenem-Resistant Bacteria, *Diagnostics*, 2023, **13**(4), 656, DOI: 10.3390/diagnostics13040656.

52 M. J. Anderson, E. Torres-Chavolla, B. A. Castro and E. C. Alocilja, One step alkaline synthesis of biocompatible gold nanoparticles using dextrin as capping agent, *J. Nanopart. Res.*, 2011, **13**(7), 2843–2851, DOI: 10.1007/s11051-010-0172-3.

53 L. Poirel, T. R. Walsh, V. Cuvillier and P. Nordmann, Multiplex PCR for detection of acquired carbapenemase genes, *Diagn. Microbiol. Infect. Dis.*, 2011, **70**(1), 119–123.

54 E. Dester, K. Kao and E. C. Alocilja, Detection of Unamplified E. coli O157 DNA Extracted from Large Food Samples Using a Gold Nanoparticle Colorimetric Biosensor, *Biosensors*, 2022, **12**(5), 274, DOI: 10.3390/bios12050274.

55 S. A. Sharief, O. Caliskan-Aydogan and E. Alocilja, Carbohydrate-coated magnetic and gold nanoparticles for point-of-use food contamination testing, *Biosens. Bioelectron.:X*, 2023, **13**, 100322.

56 B. Mondal, S. Ramlal, P. S. Lavu, N. Bhavanashri and J. Kingston, Highly sensitive colorimetric biosensor for staphylococcal enterotoxin B by a label-free aptamer and gold nanoparticles, *Front. Microbiol.*, 2018, **9**, 179, DOI: **10.3389/fmicb.2018.00179**.

57 J. Hu, K. Fu and P. W. Bohn, Whole-Cell Pseudomonas aeruginosa Localized Surface Plasmon Resonance Aptasensor, *Anal. Chem.*, 2018, **90**(3), 2326–2332, DOI: **10.1021/acs.analchem.7b04800**.

58 S. Umesha and H. M. Manukumar, Advanced molecular diagnostic techniques for detection of food-borne pathogens: Current applications and future challenges, *Crit. Rev. Food Sci. Nutr.*, 2018, **58**(1), 84–104, DOI: **10.1080/10408398.2015.1126701**.

59 J. W. F. Law, N. S. A. Mutalib, K. G. Chan and L. H. Lee, Rapid metho ds for the detection of foodborne bacterial pathogens: Principles, applications, advantages and limitations, *Front. Microbiol.*, 2015, **5**, 770, DOI: **10.3389/fmicb.2014.00770**.